1748 *Organometallics* **2009,** *28,* 1748–1757

Evaluation of the Oxygen π-Donation in Permethyltitanocene Silanolates and Alcoholates

Vojtech Varga,[†] Ivana Císařová,[‡] Róbert Gyepes,[‡] Michal Horáček,[§] Jiří Kubišta,[§] and Karel Mach[§,*]

Research Institute of Inorganic Chemistry, Revoluční 84, 400 01 Ústí nad Labem, Czech Republic, Department of Inorganic Chemistry, Charles University, Hlavova 2030, 128 40 Prague 2, Czech Republic, and J. Heyrovský Institute of Physical Chemistry, Academy of Sciences of the Czech Republic, v.v.i., Dolejškova 3, 182 23 Prague 8, Czech Republic

Received December 22, 2008

A series of compounds [$Cp^*_2Ti(III)OR'$] where R′ is $^iPr_3Si$ (**2**), Ph_3Si (**3**), $(^tBuO)_3Si$ (**4**), $(c\text{-}C_5H_9)_7Si_8O_{12}$ (**5**), and ^tBu (**6**) were prepared by protolysis of the titanium−methylene bond in singly tucked-in permethyltitanocene [$Cp^*Ti(III)(\eta^5{:}\eta^1\text{-}C_5Me_4CH_2)$] with the respective silanols or *tert*-butanol. Their electronic transitions from the ground-state molecules to their first excited states (dominantly a $1a_1 \rightarrow b_2$ transition) occur in the range 1300−1800 nm, originating from π-donation from oxygen lone pair electrons to the Ti−O bond (as found by Andersen et al. *J. Am. Chem. Soc.* **1996**, *118*, 1719). The X-ray crystal structures of **2**−**4** and **6** revealed that steric effects of substituents R′ change the geometry of the titanocene moiety only negligibly. DFT calculations of the $1a_1 \rightarrow b_2$ transition for optimized structures of **2**, **4**, **6**, [$Cp^*_2Ti(III)OH$] (**7**), and [$Cp^*_2Ti(III)OMe$] (**8**) reproduced the dependence of experimental $\lambda(1a_1 \rightarrow b_2)$ on electron donation/attraction properties of R′ and revealed that the decrease of the oxygen π-donation is accompanied with an increase in negative natural charge on the OR′ group. The observed increase of $\lambda_{exp}(1a_1 \rightarrow b_2)$ in the order of substituents R′, Me < ^tBu < H < Ph < Si^iPr_3 < $SiPh_3$ ∼ $Si(O^tBu)_3$ < $(c\text{-}C_5H_9)_7Si_8O_{12}$ (SIPOSS cluster), thus indicates the decrease of Ti−O π-interaction with an increased polarity of the Ti−O bond. The DFT calculations of **7** with the naturally bent and collinear Ti−O−H conformation showed only a small effect of bending on the oxygen π-donation.

Introduction

There is still continuous interest in exploiting silica surface hydroxyl groups for a controlled anchoring of homogeneous catalysts to obtain highly selective catalysts, which could approach the properties of, for example, single-site catalysts for the polymerization of olefins.[1] The situation with the presence of two or three cooperative or isolated SiOH groups on the silica surface has been successively modeled using polyhedral oligomeric silsesquioxanes (POSS) containing monosilanol, e.g., $(c\text{-}C_5H_9)_7Si_8O_{12}OH$ (SIPOSS), disilanol, e.g., $(c\text{-}C_5H_9)_8Si_8O_{11}(OH)_2$ (DIPOSS), and trisilanol functionalities, e.g., $(c\text{-}C_5H_9)_7Si_7O_9(OH)_3$ (TRIPOSS).[2] The use of POSS silanols for the preparation of numerous metal silanolates was reviewed,[3] and among early transition metal (Ti, Zr) POSS silanolates[4] numerous representatives were investigated as catalysts for the polymerization of olefins.[5]

In particular, single-site catalysts of the type $Cp'Ti(OR')R''_2/M(C_6F_5)_3$ became the subject of intense research, where the effect of any siloxy, aryloxy, or alkoxy ligands on the stability of ion pair bimetallic complexes and their catalytic activity was of main interest. An excellent study for Cp′ = η^5-1,3-$(SiMe_3)_2C_5H_3$, OR′ = $(c\text{-}C_5H_9)_7Si_8O_{12}O$ (SIPOSS) or Ph_3SiO, and R″ = CH_2Ph, and M = B concluded that $(c\text{-}C_5H_9)_7Si_8O_{12}OH$ is a stronger Brønsted acid than Ph_3SiOH and that the equilibrium (eq 1)

$$Cp'Ti(OR')(CH_2Ph)_2 + B(C_6F_5)_3 <===> [Cp'Ti(OR')(CH_2Ph)]^+[(CH_2Ph)B(C_6F_5)_3]^- \quad (1)$$

is shifted more to ion pairs for OR′ = $OSiPh_3$.[6] A recent study of the system for Cp′ = η^5-C_5Me_5 (Cp*), OR′ = OSi^iPr_3, R″ = Me, and M = B or Al proved that zwitterionic complexes $[Cp^*Ti(OSi^iPr_3)(Me)]^+[MeM(C_6F_5)_3]^-$ were formed and were

---

* To whom correspondence should be addressed. E-mail: mach@jh-inst.cas.cz.

[†] Research Institute of Inorganic Chemistry.

[‡] Charles University.

[§] Academy of Sciences of the Czech Republic.

(1) (a) Chien, J. C. W. In *Metallocene-Based Polyolefins*; Scheirs, J., Kaminsky, W., Eds.; John Wiley and Sons Ltd.: Chichester, England, 2000; Vol. 1, pp 173−199. (b) Hlatky, G. G. *Chem. Rev.* **2000**, *100*, 1347–1376. (c) Zecchina, A.; Groppo, E.; Bordiga, S. *Chem.−Eur. J.* **2007**, *13*, 2440–2460. (d) Millot, N.; Cox, A.; Santini, C. C.; Molard, Y.; Basset, J.-M. *Chem.−Eur. J.* **2002**, *8*, 1438–1442, and references therein.

(2) (a) Brown, J. F.; Vogt, L. H. *J. Am. Chem. Soc.* **1965**, *87*, 4313–4317. (b) Feher, F. J.; Newman, D. A.; Walzer, J. F. *J. Am. Chem. Soc.* **1989**, *111*, 1741–1748. (c) Feher, F. J.; Newman, D. A. *J. Am. Chem. Soc.* **1990**, *112*, 1931–1936. (d) Feher, F. J.; Weller, K. J. *Organometallics* **1990**, *9*, 2638–2640. (e) Edelmann, F. T. *Angew. Chem., Int. Ed. Engl.* **1992**, *31*, 586–587.

(3) (a) Duchateau, R. *Chem. Rev.* **2002**, *102*, 3525–3542. (b) Lorenz, V.; Edelman, F. T. *Adv. Organomet. Chem.* **2005**, *53*, 101–151. (c) Marciniec, B.; Maciejewski, H. *Coord. Chem. Rev.* **2001**, *223*, 301–335.

(4) (a) Feher, F. J.; Gonzales, S. L.; Ziller, J. W. *Inorg. Chem.* **1988**, *27*, 3440–3442. (b) Feher, F. J.; Walzer, J. F. *Inorg. Chem.* **1990**, *29*, 1604–1611. (c) Feher, F. J.; Budzichowski, T. A.; Rahimian, K.; Ziller, K. J. *J. Am. Chem. Soc.* **1992**, *114*, 3859–3866. (d) Edelmann, F. T.; Giessmann, S.; Fischer, A. *J. Organomet. Chem.* **2001**, *620*, 80–89. (e) Wada, K.; Itayama, N.; Watanabe, N.; Bundo, M.; Kondo, T.; Mitsudo, T. *Organometallics* **2004**, *23*, 5824–5832. (f) Fraile, J. M.; García, J. I.; Mayoral, J. A.; Vispe, E. *J. Catal.* **2005**, *233*, 90–99.

10.1021/om801209f CCC: $40.75

stable in solution for several days.[7] The systems for Cp′ = η^5-C_5H_5 (Cp), OR′ = $OC_6H_3Me_2$-2,6 or similar ligands, R″ = Me, and M = B generated zwitterionic complexes $[CpTi(OR')(Me)]^+[MeB(C_6F_5)_3]^-$; however, these were unstable in solution even at −20 °C, decomposing in two concurrent ways while eliminating methane and $MeB(C_6F_5)_2$.[8] The system for Cp′ = Cp*, OR′ = $OSi(CH_2CH_2SiMePh_2)_3$, R″ = Me, and M = B also generated the zwitterionic $[Cp^*Ti(OR')(Me)]^+[MeB(C_6F_5)_3]^-$ complex, which decomposed at room temperature with $t_{1/2} \approx 48$ h to give two decomposition products, the same as in the preceding case.[9] Apparently, the lowest stability for complexes of this type was noticed for the expected $[Cp^*Ti(O^tBu)(Me)]^+[MeB(C_6F_5)_3]^-$ complex, which decomposed immediately after mixing its precursors.[10] The complete elimination of isobutene however indicated a different decomposition pathway.[11]

Generally, in the absence of the OR′ ligand, the $[Cp^*TiMe_3]/[B(C_6F_5)_3]$ system formed a highly active catalyst for either polymerization of ethene to a high-molecular polymer or styrene to syndiotactic polystyrene when its components were mixed in the presence of monomer using nonpolar solvents.[12a] When no monomers were added, the reaction led to the formation of the anticipated zwitterionic complex $[Cp^*TiMe_2]^+[MeB(C_6F_5)_3]^-$ in an NMR tube experiment at low temperature; however, this product rapidly decomposed at room temperature and was then inactive toward olefins.[12b] Replacement of one or two Me groups with alkoxy groups led to a decrease in catalytic activity, which was attributed to the decreased electrophilicity of the metal resulting from π-electron donation of the alkoxy oxygen lone pair to the empty d orbital on the metal.[12c] The application of the C_6F_5 or OC_6F_5 ligands as poor π-electron donor OR′ moieties yielded thermally unstable zwitterionic complexes with $B(C_6F_5)_3$.[12d] Thus, the only monocyclopentadienyltitanium complexes of this type characterized by crystallography are the catalytically inactive zwitterionic complexes $[Cp^*Ti(OR')_2]^+[MeB(C_6F_5)_3]^-$, where R′ = ^{t}Bu[10] or ^{i}Pr, the complex containing O^{i}Pr ligands being thermally less stable.[13] The methyl carbon atom was σ-bonded to boron, and two hydrogen atoms of the methyl group exerted an agostic interaction[14] with the titanium atom, similarly to known zirconocene zwitterionic complexes.[15]

The extent of the stabilizing effect of the OR′ group in $Cp'Ti(OR')R''_2/M(C_6F_5)_3$ systems has been discussed in terms of Brønsted acidity of corresponding POSS silanols[16] or a pair of SIPOSS and Ph_3SiOH,[6] different silylation rates of POSS silanols,[2c] and reactivities of silanols, phenols, or alcohols in protolysis reactions, e.g., with $[Zr(CH_2Ph)_4]$,[5a] $[Cp'Ti(CH_2Ph)_3]$,[5b] or $[Cp^*TaMe_4]$,[17a] or exchange reactions, e.g., $(^tBuO)_3SiOH$ with $Ta(O^iPr)_5$,[17b] or Ph_3SiOH with $[Ti(O^tBu)_4]$,[17c] which were based mostly on a qualitative observation.

In this contribution we compare the ability of silanolate groups $(c\text{-}C_5H_9)_7Si_8O_{12}O$ (SIPOSS), $(^tBuO)_3SiO$, Ph_3SiO, and $^iPr_3SiO$ and ^{t}BuO, MeO, PhO, and OH groups to act in π-donation of a lone electron pair from oxygen to the Ti−O bond. Bis(pentamethylcyclopentadienyl)titanium(III) oxy derivatives are used as model compounds with a uniform structure of the titanocene moiety for determination of energy of the $1a_1 \rightarrow b_2$ transition in their electronic absorption spectra, which is the inherent measure of the effect.[18] Crystal structures and density functional theory (DFT) calculations of the model compounds support the applicability of the method.

Results and Discussion

Compounds $[Cp^*_2TiOR']$ where R′ is $^iPr_3Si$ (**2**), Ph_3Si (**3**), $(^tBuO)_3Si$ (**4**), $(c\text{-}C_5H_9)_7Si_8O_{12}$ (**5**), and ^{t}Bu (**6**) were prepared by silanolysis or alcoholysis of the titanium−methylene bond in singly tucked-in permethyltitanocene $[Cp^*Ti(III)(\eta^5{:}\eta^1\text{-}C_5Me_4CH_2)]$ (**1**)[19] with the respective silanols or *tert*-butanol in a practically quantitative reaction (Scheme 1).

---

(5) (a) Duchateau, R.; Abbenhuis, H. C. L.; van Santen, R. A.; Meetsma, A.; Thiele, S. K.-H.; van Tol, M. F. H. *Organometallics* **1998**, *17*, 5663–5673. (b) Duchateau, R.; Abbenhuis, H. C. L.; van Santen, R. A.; Thiele, S. K.-H.; van Tol, M. F. H. *Organometallics* **1998**, *17*, 5222–5224. (c) Kim, Y.; Han, Y.; Lee, M. H.; Yoon, S. W.; Choi, K. H.; Song, B. G.; Do, Y. *Macromol. Rapid Commun.* **2001**, *22*, 573–578. (d) Severn, J. R.; Duchateau, R.; van Santen, R. A.; Ellis, D. D.; Spek, A. L. *Organometallics* **2002**, *21*, 4–6. (e) Metcalfe, R. A.; Kreller, D. I.; Tian, J.; Kim, H.; Taylor, N. J.; Corrigan, J. F.; Collins, S. *Organometallics* **2002**, *21*, 1719–1726.

(6) Duchateau, R.; Cremer, U.; Harmsen, R. J.; Mohamud, S. I.; Abbenhuis, H. C. L.; van Santen, R. A.; Meetsma, A.; Thiele, S. K.-H.; van Tol, M. F. H.; Kranenburg, M. *Organometallics* **1999**, *18*, 5447–5459.

(7) Postigo, L.; Vázquez, A. B.; Sánchez-Nieves, J.; Royo, P.; Herdtweck, E. *Organometallics* **2008**, *27*, 5588–5597.

(8) Phomphrai, K.; Fenwick, A. E.; Sharma, S.; Fanwick, P. E.; Caruthers, J. M.; Delgass, W. N.; Abu-Omar, M. M.; Rothwell, I. P. *Organometallics* **2006**, *25*, 214–220.

(9) Amo, V.; Andrés, R.; de Jesús, E.; de la Mata, F. J.; Flores, J. C.; Gómez, R.; Gómez-Sal, M. P.; Turner, J. F. *Organometallics* **2005**, *24*, 2331–2338.

(10) Pinkas, J.; Varga, V.; Císařová, I.; Gyepes, R.; Horáček, M.; Mach, K. *J. Organomet. Chem.* **2007**, *692*, 2064–2070.

(11) (a) Stoebenau, E. J.; Jordan, R. F. *J. Am. Chem. Soc.* **2006**, *128*, 8162–8175. (b) Jordan, A. Y.; Meyer, T. Y. *J. Organomet. Chem.* **1999**, *591*, 104–113.

(12) (a) Gillis, D. J.; Tudoret, M.-J.; Baird, M. C. *J. Am. Chem. Soc.* **1993**, *115*, 2543–2545. (b) Wang, Q.; Gillis, D. J.; Quyoum, R.; Jeremic, D.; Tudoret, M.-J.; Baird, M. C. *J. Organomet. Chem.* **1997**, *527*, 7–14. (c) Wang, Q.; Quyoum, R.; Gillis, D. J.; Tudoret, M.-J.; Jeremic, D.; Hunter, B. K.; Baird, M. C. *Organometallics* **1996**, *15*, 693–703. (d) Sarsfield, M. J.; Ewart, S. W.; Tremblay, T. L.; Roszak, A. W.; Baird, M. C. *J. Chem. Soc., Dalton Trans.* **1997**, 3097–3104.

(13) Varga, V.; Pinkas, J.; Císařová, I.; Gyepes, R.; Mach, K.; Kubišta, J.; Horáček, M. *Collect. Czech. Chem. Commun.* **2008**, *73*, 1161–1176.

(14) (a) Brookhart, M.; Green, M. L. H. *J. Organomet. Chem.* **1983**, *250*, 395–408. (b) Braga, D.; Grepioni, F.; Tedesco, E.; Biradha, K.; Desiraju, G. R. *Organometallics* **1997**, *16*, 1846–1856. (c) Thakur, T. S.; Desiraju, G. R. *Chem. Commun.* **2006**, *552*, 555.

(15) (a) Beck, S.; Prosenc, M. H.; Brintzinger, H.-H.; Goretzki, R.; Herfert, N.; Fink, G. *J. Mol. Catal. A* **1996**, *111*, 67–79. (b) Beck, S.; Lieber, S.; Schaper, F.; Geyer, A.; Brintzinger, H.-H. *J. Am. Chem. Soc.* **2001**, *123*, 1483–1489. (c) Yang, X.; Stern, C. L.; Marks, T. J. *J. Am. Chem. Soc.* **1994**, *116*, 10015–10031.

(16) (a) Dijkstra, T. W.; Duchateau, R.; van Santen, R. A.; Meetsma, A.; Yap, G. P. A. *J. Am. Chem. Soc.* **2002**, *124*, 9856–9864. (b) Liu, H.; Kondo, S.-I.; Tanaka, R.; Oku, H.; Unno, M. *J. Organomet. Chem.* **2008**, *693*, 1301–1308.

(17) (a) Sánchez-Nieves, J.; Royo, P. *Organometallics* **2007**, *26*, 2880–2884. (b) Brutchey, R. L.; Lugmair, C. G.; Schebaum, L. O.; Tilley, T. D. *J. Catal.* **2005**, *229*, 72–81. (c) Johnson, B. F. G.; Klunduk, M. C.; Martin, C. M.; Sankar, G.; Teate, S. J.; Thomas, J. M. *J. Organomet. Chem.* **2000**, *596*, 221–225.

(18) Lukens, W. W., Jr.; Smith, M. R., III; Andersen, R. A. *J. Am. Chem. Soc.* **1996**, *118*, 1719–1728.

(19) (a) Bercaw, J. E. *J. Am. Chem. Soc.* **1974**, *96*, 5087–5095. (b) Pattiasina, J. W. Ph.D.Thesis, University of Groningen, Groningen, The Netherlands, 1988; pp 35−77. (c) Pinkas, J.; Císařová, I.; Gyepes, R.; Horáček, M.; Kubišta, J.; Čejka, J.; Gŏmez-Ruiz, S.; Hey-Hawkins, E.; Mach, K. *Organometallics* **2008**, *27*, 5532–5547, and references therein.

(20) (a) Crocker, M.; Herold, R. H. M.; Orpen, A. G.; Overgaag, M. T. A. *J. Chem. Soc., Dalton Trans.* **1999**, 3791–3804. (b) Moran, P. D.; Bowmaker, G. A.; Cooney, R. P.; Finnie, K. S.; Bartlett, J. R.; Woolfrey, J. L. *Inorg. Chem.* **1998**, *37*, 2741–2748.

(21) (a) Horáček, M.; Gyepes, R.; Kubišta, J.; Mach, K. *Inorg. Chem. Commun.* **2004**, *7*, 155–159. (b) Horáček, M.; Císařová, I.; Čejka, J.; Karban, J.; Petrusová, L.; Mach, K. *J. Organomet. Chem.* **1999**, *577*, 103–112.

(22) Luinstra, G. A.; ten Kate, L. C.; Heeres, H. J.; Pattiasina, J. W.; Meetsma, A.; Teuben, J. H. *Organometallics* **1991**, *10*, 3227–3237.

(23) (a) Wolff von Gudenberg, D.; Kang, H.-C.; Massa, W.; Dehnicke, K.; Maichle-Mössmer, C.; Strähle, J. *Z. Anorg. Allg. Chem.* **1994**, *620*, 1719–1724. (b) Crocker, M.; Herold, R. H. M.; Orpen, A. G. *Chem. Commun.* **1997**, 2411–2412. (c) Menge, W. M. P. B.; Verkade, J. G. *Inorg. Chem.* **1991**, *30*, 4628–4631.

Scheme 1

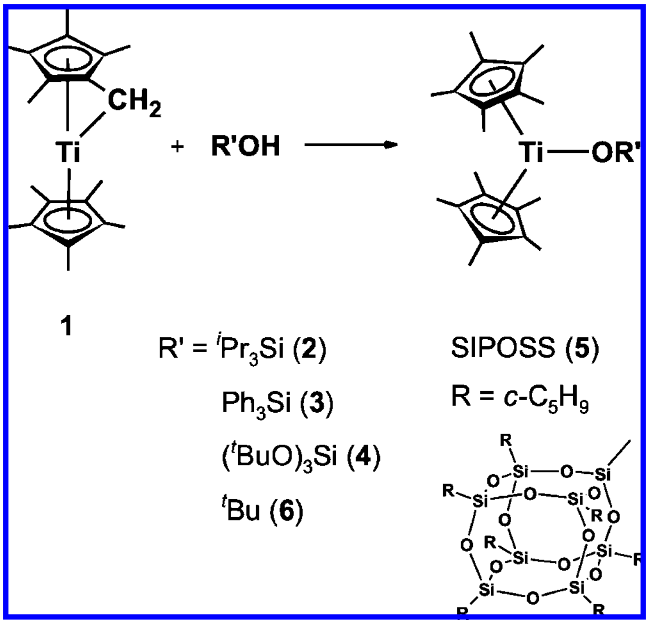

This synthetic method was used by Pattiasina for obtaining **6**[19b] and by Edelmann et al.[4d] to prepare a SIPOSS compound similar to **5**. All compounds except **5** were characterized by single-crystal X-ray diffraction analysis and EI-MS, and all compounds by IR, UV-near IR, and EPR spectra. The EI-MS spectra displayed abundant molecular ions for all compounds, and their fragmentation was consistent with their molecular structures. The fragment ions arising from elimination of Cp* were base peaks for **2** and **3**, whereas for **6**, the $[M - R'OH]^+$ ion was the base peak and the next most abundant ion was $[M - Cp^*]^+$. The molecular ion of **4** successively eliminated butene molecules and Cp*, giving a base peak of the composition $[Cp^*TiOSi(OH)_3]^+$. Thus the titanocene siloxides **2**−**4** upon ionization preferred the loss of the Cp* ligand compared to the alkoxide **6** with overwhelming dissociation of the alcohol. In the infrared spectra, only the most intense absorption bands were tentatively assigned. The valence Si−O(Ti) vibration was assigned to the band at 897 cm^{-1} for **2**, 956 cm^{-1} for **3**, 1025 cm^{-1} for **4**,[20a] and 1038 cm^{-1} for **5**. The skeletal Si−O−Si vibrations in **5** at 1117 cm^{-1} did not differ from that in SIPOSS, and in **4**, the bands at 1047 and 964 cm^{-1} were attributed to ν(Si−O(C)) and ν(C−O(Si)) vibration, respectively. The band at 985 cm^{-1} for **6** is the valence C−O vibration coupled with ν(Ti−O),[20b] and the typical absorption bands for *tert*-butyl groups in **4** and **6** should be those at 1192 and 1182 cm^{-1}, respectively. The EPR spectra form typically a very narrow single line (ΔH ~2.4−2.8 G) in the range $g = 1.971-1.978$ flanked by about 20-times less intense multiplets due to ^{49}Ti ($I_N = 7/2$) and ^{47}Ti ($I_N = 5/2$) with $a_{Ti} = 8.2-8.8$ G. The electronic absorption spectra of **2**−**6** displayed three well-observable bands in the regions 497−525, 605−665, and 1300−1800 nm. Among these, the absorption band of the lowest energy transition can indicate the presence and the extent of π-donation ability of oxygen to the Ti−O bond.

According to the qualitative MO diagram developed by Andersen et al.[18] (Figure 1) for $[(\eta^5\text{-}C_5Me_5)_2Ti(III)X]$ d^1 complexes, where X was an element with a lone electron pair in the p orbital, the transition from the SOMO orbital, essentially d_{z^2} perpendicular to the Cg−Ti−Cg (Cg is the centroid of gravity of the cyclopentadienyl ring) plane, to the empty orbital d_{xz} becomes observable when the latter is destabilized by interaction with the electron pair in the p_z orbital of X. The $1a_1 \rightarrow b_2$ transition has been observed at $\lambda < 2000$ nm for X = F, NH_2, NHMe, OMe, OPh,[18] OH,[21a] and $[(\eta^5\text{-}C_5HMe_4)_2Ti(III)(O^tBu)]$.[21b] The wavelengths of the $1a_1 \rightarrow b_2$ transition for compounds **2**−**6** and literature data for similar compounds $[Cp^*_2Ti(III)OH]$ (**7**),[21a] $[Cp^*_2Ti(III)OMe]$ (**8**), and $[Cp^*_2Ti(III)OPh]$ (**9**)[18] are given in Table 1. These spectroscopic data will be correlated with the X-ray structure data for **2**−**4**, **6**, and **7** and computed optimized structure data and the $1a_1 \rightarrow b_2$ transition thereof for **2**, **4**, and **6**−**8** (see below).

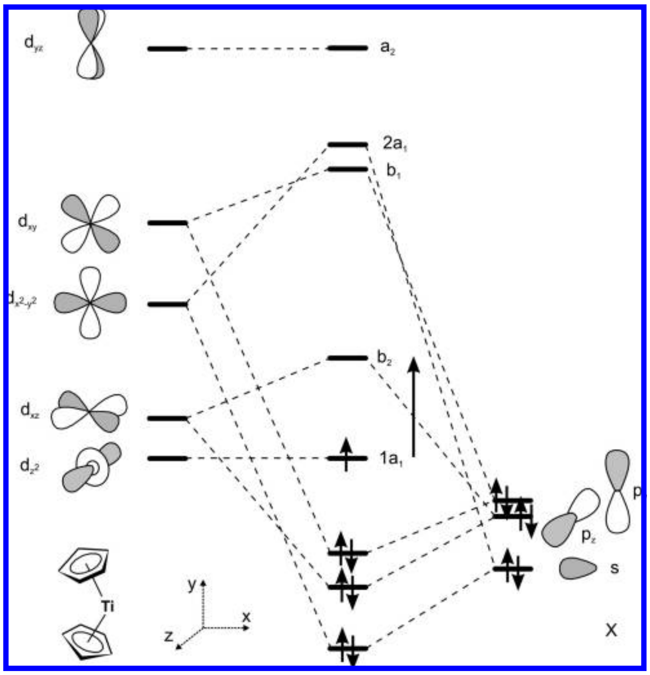

Figure 1. Qualitative MO diagram for a bent titanocene after Andersen et al.[18] showing the generation of one σ, two π, and one singly occupied nonbonding orbital.

Crystal Structures of 2−4 and 6. All the compounds studied with the exception of **5** afforded suitable single crystals for X-ray diffraction analysis. Data collection for these studies was carried out on the same instrument within two months, minimizing thus any data collection differences. The geometric parameters common to all compounds are listed in Table 2, and the PLATON drawings of compounds **2**−**4** and **6** are shown in Figures 2−5.

The data prove that geometry of the titanocene moiety is very similar for all the compounds, differing by a maximum of 3.1° in the Cg(1)−Ti−Cg(2) angle. The sum of this angle with the Cg(1)−Ti−O and Cg(2)−Ti−O ones makes 360° within esd's, confirming thus a trigonal-planar coordination environment around the titanium atom. The value of the Cg(1)−Ti−Cg(2) angle indicates a degree of steric congestion on the open side of the permethyltitanocene shell caused by bulkiness of the OR′ ligand; the smaller the ligand, the larger the angle contained. Surprisingly, the largest value of Cg(1)−Ti−Cg(2) in Table 2 indicates the smallest steric congestion for **3**, which is similar to that in $[Cp^*_2Ti(III)CH_2CMe_3]$, showing an angle of 139.4(3)°.[22] Listings of intramolecular nonbonding contacts between the OR′ ligands and permethylcyclopentadienyl ligands revealed that the most pronounced repulsions are those between the oxygen atom O(Ti) and the cyclopentadienyl ring carbon atoms C(1), C(2), C(11), and C(12), as all the compounds had three contact distances O···C shorter than the sum of covalent radii (3.22 Å) by 0.36−0.20 Å. However, the hydroxyl

Table 1. Experimental First Excitation (Dominantly $1a_1 \rightarrow b_2$ Transition) Wavelengths (nm) for 2−9 and Calculated First Excitation Wavelengths, Natural Charges on the Cp$_2$*Ti Moiety, Sum of α and β Delocalization Energies O(p$_z$)→Ti (kcal/mol), Optimized O−Z (Z = C, Si, or H) Distances (Å), and Optimized Ti−O−Z Angles (deg) for 2, 4, and 6−8

	5	4	3	2	6	7	8	9
$\lambda_{exp}(1a_1 \rightarrow b_2)$	1800	1700	1725	1585	1300	1477[a]	1282[b]	1528[b]
$\lambda_{calc}(1a_1 \rightarrow b_2)$		1451		1219	1069	1253(1224)[c]	1087(1081)[c]	
$q_{natural}$ Cp$_2$*Ti		0.607		0.570	0.452	0.470	0.467	
E_{deloc}(O(p$_z$)→Ti)		24.96		25.22	32.65	31.68	34.45	
d(Ti−O)		1.953		1.930	1.876	1.893	1.853	
d(O-Z)		1.629		1.669	1.421	0.967	1.392	
∠Ti−O−Z		175.36		171.14	177.17	121.96	166.51	

[a] Taken from ref 21a. [b] Taken from ref 18. [c] Data in parentheses are for the collinear arrangement of Ti−O−H or Ti−O−C.

Table 2. Selected Bond Lengths and Bond Angles for 2−4, 6, and 7[a]

	4	3	2 (mol. 1)	2 (mol. 2)	6	7
			Bond Lengths (Å)			
Ti−Cg(1)[b]	2.0867(7)	2.0928(10)	2.092(2)	2.106(2)	2.1137(6)	2.070(1)
Ti−Cg(2)[b]	2.0878(7)	2.0850(9)	2.107(2)	2.101(2)	2.1179(7)	2.068(1)
Ti−Pl(1)[b]	2.0863(2)	2.0917(3)	2.0911(7)	2.1049(7)	2.1136(2)	
Ti−Pl(2)[b]	2.0873(2)	2.0848(3)	2.1061(7)	2.0980(7)	2.1164(2)	
Ti−O	1.9244(9)	1.9190(13)	1.919(3)	1.924(3)	1.8658(9)	1.889(2)
Si−O(Ti)	1.6032(9)	1.6115(13)	1.638(3)	1.637(3)	1.4137(15)[c]	
			Bond Angles (deg)			
Cg(1)−Ti−Cg(2)	138.30(3)	139.16(4)	136.34(8)	135.84(8)	136.04(3)	143.79(5)
Cg(1)−Ti−O	111.08(4)	111.69(5)	110.12(10)	111.22(10)	111.09(4)	109.84(9)
Cg(2)−Ti−O	110.59(4)	109.10(5)	113.54(10)	112.93(10)	112.86(4)	106.36(9)
Ti−O−Si	176.89(6)	173.50(8)	172.48(17)	174.99(18)	174.34(9)[d]	
φ[e]	39.28(6)	38.47(9)	40.33(12)	41.00(12)	41.24(5)	35.06(12)

[a] Taken from ref 21a. [b] Cg(1) and Cg(2) are centroids and Pl(1) and Pl(2) least-squares planes of the C(1−5) and C(11−15) cyclopentadienyl rings, respectively. [c] Distance O−C(21). [d] Angle Ti−O−C(21). [e] Dihedral angle between the least-squares planes of cyclopentadienyl rings.

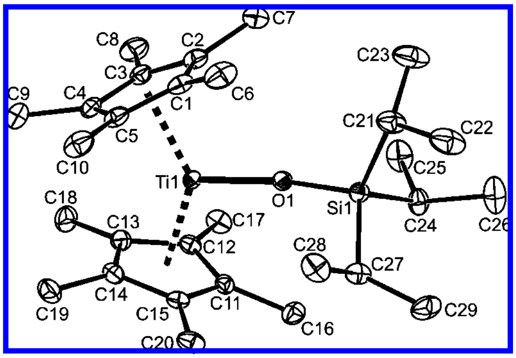

Figure 2. PLATON[45] drawing of **2** at the 30% probability level with atom-labeling scheme. Hydrogen atoms are omitted for clarity.

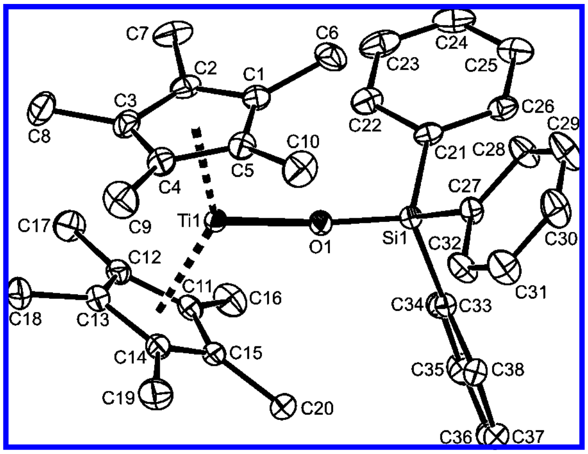

Figure 3. PLATON[45] drawing of **3** at the 30% probability level with atom-labeling scheme. Hydrogen atoms are omitted for clarity.

compound [Cp*$_2$Ti(III)OH] (**7**), whose parameters are included for comparison in Table 2, showed a larger Cg(1)−Ti−Cg(2) angle (143.79(5)°),[21a] which indicates that the presence of R′ groups decreases the Cg(1)−Ti−Cg(2) angle. The methyl carbon atoms on the cyclopentadienyl ligands are in general deviated from the least-squares plane of the ring away from titanium, most remarkably on the closed shell side, for the methyls in hinge position close to the Cg(1), Ti, Cg(2) plane. The maximum deviation was in the range 0.42−0.44 Å for all compounds except **3**, where the maximum deviation of 0.370(4) Å was found for C(18). This steric congestion on both sides of the titanocene shell results in only negligible tilting of the cyclopentadienyl rings (see the slightly smaller Ti−Pl (Pl is the least-squares plane of Cp* ring) distances compared to Ti−Cg ones in Table 2). The Ti−O bond length in **6** was markedly shorter and the average Ti−Cg distance slightly longer than in the siloxy compounds, where these parameters differed rather negligibly. The effect of siloxy substituents was discernible on the Si−O(Ti) bond, which was shortened in the order 2 > 3 > 4 (Table 2). The Ti−O−Si and Ti−O−C bond systems undergo only some slight bending, with angles at the oxygen atom spanning from 172.48(17)° for molecule 1 of **2** to 176.89(6)° for **4** (Table 2). The angle magnitude is apparently controlled by intramolecular packing demands; for example, in [Cp$_2$Ti(Cl)OSiPh$_3$] the Ti−O−Si angle was 164.5(2)°.[23a] The linear Ti−O−Si arrangement was found in tripodal complexes (−O−)$_3$TiOSiR$_3$ with (−O−)$_3$ being a TRIPOSS ligand and R = Me[20a,23b] or a titanatrane with R = Ph.[23c] Also the structure of [Ti(OSiPh$_3$)$_4$] falls into this group of compounds with three equally bent tripodal ligands (148.2(3)°) and a linear one. It is of interest that the Ti−O bond of the latter is longer (1.798(7) Å) and the Si−O bond shorter (1.613(7) Å) than the bonds in the three equal bent ligands (Ti−O 1.782(4) Å and Si−O 1.650(4) Å).[17c] The Ti−O−C bond system apparently prefers a bent arrangement. In [(η^5-C$_5$HMe$_4$)$_2$Ti(III)(O^{t}Bu)], where the Cg(1)−Ti−Cg(2) angle 136.7(1)° is close to that of **6** because one cyclopentadienyl ring is oriented with its proton-bearing carbon atom to a

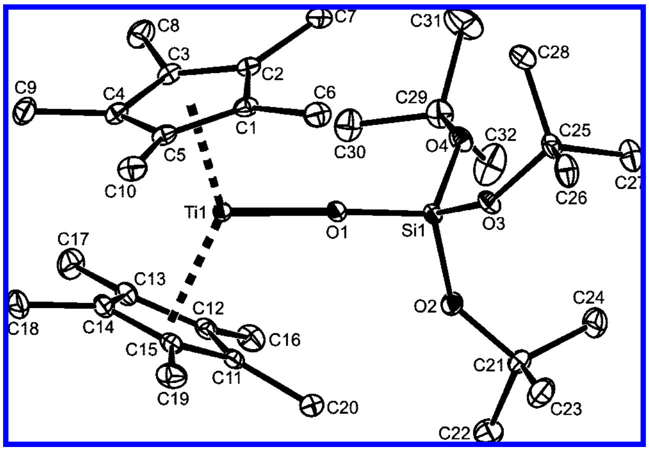

Figure 4. PLATON[45] drawing of **4** at the 30% probability level with atom-labeling scheme. Hydrogen atoms are omitted for clarity.

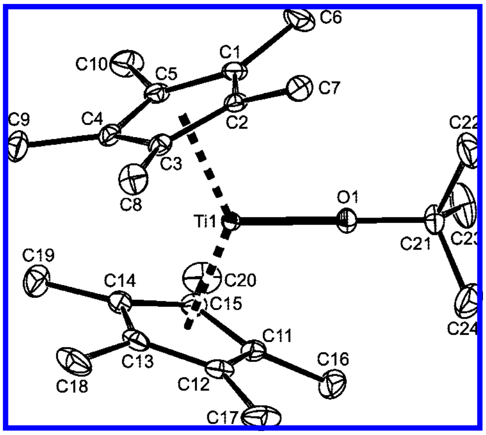

Figure 5. PLATON[45] drawing of **6** at the 30% probability level with atom-labeling scheme. Hydrogen atoms are omitted for clarity.

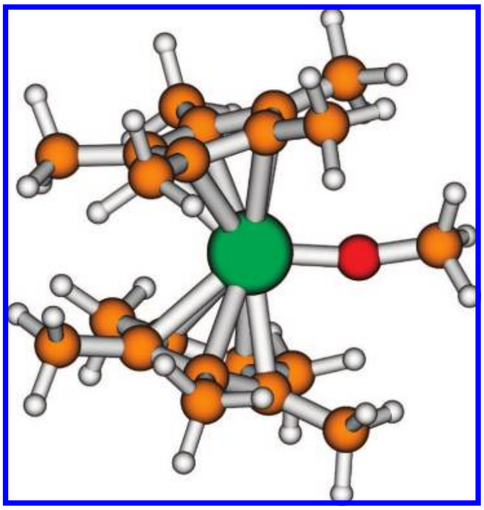

Figure 6. Optimized geometric parameters for **8**: Ti−Cg av 2.10 Å, Ti−O 1.853 Å, C−O 1.392 Å, Cg−Ti−Cg 141.78, and Ti−O−C angle 166.51°.

hinge position and the other to the O^{t}Bu group, the Ti−O−C angle (162.16(13)°) is smaller than in **6**, utilizing the space of the missing methyl group.[21b] In a number of alkoxy and aryloxy Ti(IV) complexes [$Cp_2TiCl(OR)$] (R = aryl)[24a] and [$(\eta^5\text{-}C_5H_4SiMe_3)_2TiCl(OR)$] (R = CH_2-ferrocenyl or aryl)[24b] and in sterically nonhindered [$Cp_2TiCl(OEt)$)][24c] the Ti−O−C angles were in the range 130−150°. The extremely small Ti−O−H angle of 112(4)° found for **7**[21a] was optimized to 121.9° by DFT structure optimization (see below), close to the crystallographic values for [$Cp^*_2Ti(OH)_2$],[25a] [$Cp^*_2Ti(OH)(CCPh)$],[25b] and [$Cp^*_2Ti(OH)(H_2O)$]$^+$[BPh_4]$^-$.[25c] In **4**, where the Si−O−C bond systems are not sterically hindered, their average bending was 137.02(9)°, average Si−O bond length 1.6307(10) Å, and average O−C bond length 1.4415(17) Å. The closely related compound **5**, whose crystal structure could not be determined, apparently would fall into the above-outlined trend of keeping a constant Ti−O bond length and shortening of the Si−O(Ti) bond length since the similar compound [Cp^*_2TiOR'] with R′ being $(cyclohexyl)_7Si_7O_9(OSiMe_3)_2$ (TriPOSS with two trimethylsilylated hydroxyl groups) exerted a Ti−O bond length of 1.927(2) Å and Si−O(Ti) of 1.595(2) Å.[4d]

DFT Calculations. The structures of compounds **2**, **4**, and **6**−**8** were optimized using the crystallographic parameters as input data except for **8**, where the crystallographic data for **6** were modified by replacing the *tert*-butyl group with a methyl group. The optimized geometric parameters for **2**, **4**, **6**, and **7** differed systematically from crystallographic ones showing slightly longer Ti−O, Si−O, and C−O bonds and similar Ti−O−Si or Ti−O−C angles (cf. Tables 1 and 2). The systematic elongation of the above bonds resulted presumably from a larger steric congestion in the optimized molecules that was caused by a notable elongation of all C−H bonds due to the temperature dependence of ideal hydrogen positions to cope with libration in the solid state.

The optimized structure **8** (Figure 6) showed slightly shorter Ti−O and O−C bond lengths compared to those of optimized **6**, while the Ti−O−C angle was coplanar with the Cg−Ti−Cg angle plane and was smaller compared to that of optimized **6**. The computed $1a_1 \rightarrow b_2$ transitions for all the optimized structures showed a systematic shift to shorter wavelengths by 200−250 nm from the experimental values; however, the effect of substituents R′ on band positions could be reproduced within both series. Compared with the hydroxyl hydrogen in compound **7**, the electron-donating methyl and *tert*-butyl substituents in **8** and **6** shifted the experimental as well as computed $1a_1 \rightarrow b_2$ transition to shorter wavelengths, whereas the opposite effect was unequivocally established for the computed $1a_1 \rightarrow b_2$ transition of siloxy compounds **2** and **4** and experimental spectra of **2**−**5** and **9** (see Table 1). The discrepancy between experimental and calculated transition energies could be caused by numerical difficulties arising from the treatment of systems with a low HOMO−LUMO separation; more advanced multiconfigurational methods however could not be employed due to the prohibitive size of the complexes under study.

The generally known electron-donating/attracting effects of substituents R′ primarily influence polarity of the Ti−O bond. The ionic nature of the $Cp^*_2Ti(III)OR'$ compounds is visualized for **7** by distribution of electrostatic potential (Figure 7), and the Ti−O bond polarity is reflected in natural charges on the Cp^*_2Ti moiety (Table 1). These values, ranging from 0.452 for **6** to 0.607 for **4**, would reach the limit of 1.0 for the free ion $Cp^*_2Ti^+$. Provided the structure of the Cp^*_2Ti moiety is virtually constant, the same negative charges have to be induced on the OR′ counterpart of the complexes. The absolute values of natural charges in Table 1 thus reflect the effect of R′ on the Ti−O bond polarity. The largest ionic contribution to the Ti−O bond is found for **4**, and an even higher ionic contribution is to be expected for **5** with the yet more polarized $Ti{-}O{-}Si(OSi(R)O)_3$ moiety.

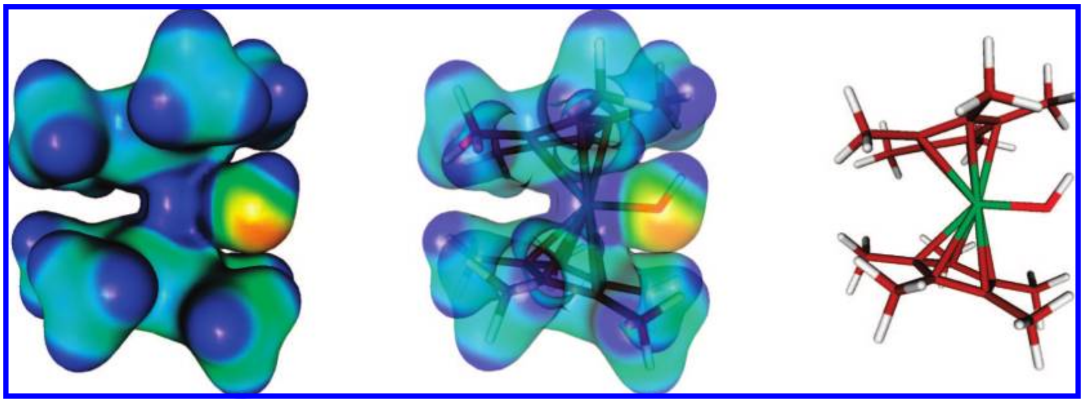

Figure 7. Isodensity surface (2%) color-coded with the electrostatic potential (left) and orientation of the molecule **7** within the isodensity surface (center), and molecule **7** (right). Color values for the electrostatic potential: blue >0.10, light blue 0.05, green 0.00, yellow −0.05, red <−0.20.

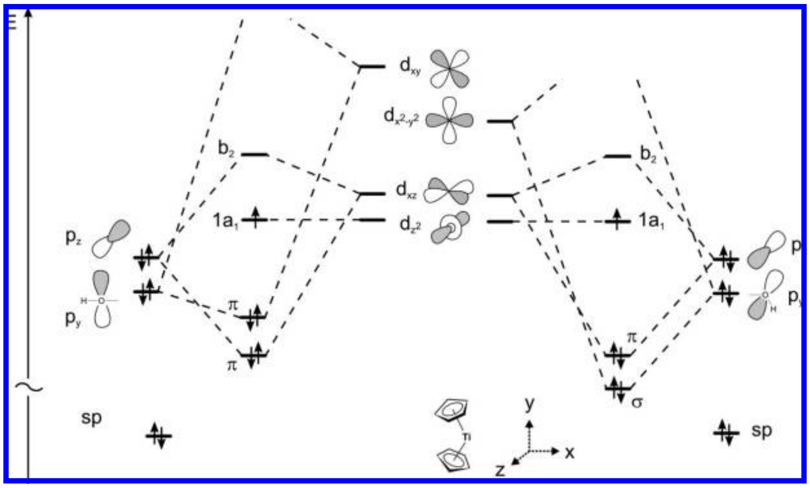

Figure 8. Correlation diagram for **7** with the collinear (left) and bent (right) Ti−O−H conformation.

A quantitative evaluation of covalent contributions was carried out by means of natural bond analysis. Due to the prevalence of the electrostatic attraction between the bent Cp*$_2$Ti moiety and the O-R groups, the default NBO search reported only lone pairs on the oxygen atoms. At the second-order donor−acceptor perturbation level the delocalization energies from the oxygen p_z lone pair to the non-Lewis metallic lone pairs followed the changes of the first excitation energies. The acceptor orbital for the oxygen p_z is the d_{xy} orbital on the metal, resulting in a neat π-interaction. The delocalization energies O(p_z)→Ti follow the reverse trend of natural charges (Table 1), in agreement with the anticipated assumption that the more polar the Ti−O bond, the weaker the covalent interaction. A direct comparison of the σ-contributions to the Ti−O bonding would be inappropriate, due to the entirely different genesis of the Si−O bond in comparison with the "regular" C−O and H−O σ-bonds. The third-row silicon atom achieves its bonding through the formation of σ* orbitals. In this type of bonding, the inductive effects play a nonanticipated important role.[26]

To understand the nature and extent of the covalent contribution to the Ti−O bonding, an interaction diagram was devised for the simplest compound, **7**, in its optimized bent (121.96°) and collinear Ti−O−H conformation using Counterpoise DFT[27] (Figure 8).

This type of calculation allows the examination of frontier orbitals not only for the real complex itself but also for its constituting fragments, chosen to be Cp*$_2$Ti$^+$ and OH$^-$ in the present case. For both conformations the SOMO $1a_1$ orbital of the complex is a nearly pure d_{z^2}, incapable of providing a good overlap with any of the ligand orbitals, and the LUMO b_2 arises from interaction of the lone electron pair in the p_z oxygen orbital, which overlaps with the empty d_{xz} orbital of titanium, as found by Andersen et al.[18] (Figure 1). For the bent conformation, the corresponding bonding orbital is HOMO and the π-bonding character of the Ti−O bond is well observable in Figure 9. In distinction to a correlation diagram in Figure 1, the σ-bond represented by the next lower orbital arises from the $d_{x^2-y^2}$ orbital overlapping with the other electron lone pair of oxygen, which is close in energy (Figure 9, left). The oxygen sp orbital binding

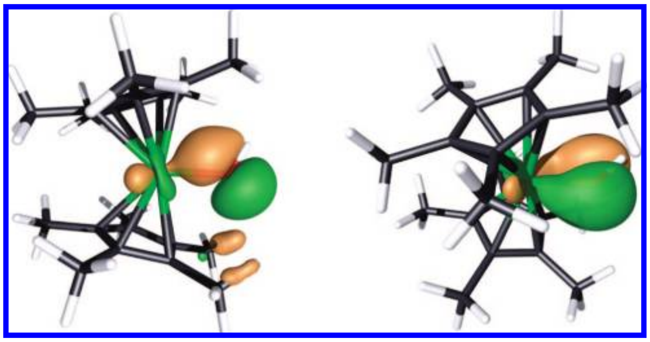

Figure 9. The σ- (left) and the π-coordination in **7**. Both molecular orbitals are doubly occupied. Orbital contours are plotted at the 5% probability level.

Figure 10. Ti−O π-bonding in the collinear **7** arising from interaction of d_{xy} and p_y orbitals (left) and d_{xz} and p_z orbitals (right). Both molecular orbitals are doubly occupied. Orbital contours are plotted at the 5% probability level.

the hydroxyl group lies too low in energy to provide an effective interaction with the $d_{x^2-y^2}$ orbital (Supporting Information, extended correlation diagram, listing of relevant orbitals and MO energies).

A collinear Ti−O−H arrangement rotates the orbital orientation on the oxygen atom directing the O−H sp hybrid orbital exactly toward the metallic center (Figure 8, left). Although this hybrid orbital has in principle a proper shape for mixing with the metal $d_{x^2-y^2}$ orbital, their actual overlap is prevented by the large energy separation of the fragment orbitals. The only remaining possible interaction for the oxygen lone electron pair in the p_y orbital is with the d_{xy} orbital. Thus a weak π-bond is formed that is orthogonal to the other π-bond, which is now lower in energy (Figure 10). This formation of a π orbital instead of a σ one results in weakening of the Ti−O bond. It is evidenced by the decrease of the calculated Ti−O Mayer bond order from 1.1 for the bent conformation to 0.6 for the collinear one, while the Mayer bond order for the O−H bond remains unchanged (0.8). As concerns the $\lambda_{calc}(1a_1 \rightarrow b_2)$, the conformation of the Ti−O−H angle has only a small effect (see Table 1) since the overlap of p_z and d_{xz} orbitals is affected negligibly by the angle change. A total energy difference for the bent and collinear **7** was found to be only 6.60 kcal/mol.

Although not accessible experimentally, the generally reiterated statement that the oxygen π-donation effect should be enhanced with the linear conformation of the Ti−O−C system[24,28] was investigated in detail by DFT computations for compound **8**. The optimized molecule of **8** with the Ti−O−C angle of 166.5° and with the linear one yielded a Mayer bond order of 1.3 for the bent conformer and 1.2 for the collinear one and a $\lambda_{calc}(1a_1 \rightarrow b_2)$ of 1087 and 1081 nm, respectively (Table 1). These values indicate that a linear arrangement only slightly enhances the lone pair π-donation effect, in agreement with the results for **7**.

For the actually studied compounds with the solid-state Ti−O−C angle of >170° the $\lambda_{exp}(1a_1 \rightarrow b_2)$ values are pertinent rather to a collinear conformation due to the solution averaging; however, the above investigation of bent and collinear conformations of **7** and **8** proved that the difference in $\lambda_{exp}(1a_1 \rightarrow b_2)$ and $\lambda_{calc}(1a_1 \rightarrow b_2)$ cannot account for the different bending in solution and in the solid state. A low sensitivity of $\lambda_{exp}(1a_1 \rightarrow b_2)$ to the Ti−O−C angle was recently confirmed by observation that the tethered alkoxy compounds **10** and **11** from Chart 1, which both have Ti−O−C angles of 133°, displayed absorption bands at 1365 and 1500 nm, respectively.[29] It is highly probable that the red shift in **11** with respect to **10** is caused by the presence of the aryl substituent; however, it is not clear whether the red shift of only 65 nm for **10** with respect to **6** (1300 nm) is caused by the smaller Ti−O−C angle or by other factors, e.g., the remote attachment of its carbon atom to an aromatic cyclopentadienyl ring.

Conclusions

The first electronic absorption band of $[Cp^*_2Ti(III)OR']$ compounds **2**−**9** in the near-infrared region is suitable for detection of the oxygen π-donation effect and evaluation of its extent. The absorption band was assigned to the $1a_1 \rightarrow b_2$ transition, whose energy was proportional to the magnitude of the oxygen π-donation.[18] The X-ray diffraction analysis of compounds **2**−**4** and **6** revealed that steric effects of substituents R′ change the geometry of the titanocene moiety only negligibly, and hence, the oxygen π-donation effect is controlled by the electron donation/attraction effect of substituent R′ via a decrease/increase of the Ti−O bond polarity. According to $\lambda_{exp}(1a_1 \rightarrow b_2)$ for **2**−**9**, occurring in the range 1280−1800 nm, the oxygen π-donation decreased in the order of substituents Me > ^{t}Bu > H > Ph > Si^{i}Pr$_3$ > SiPh$_3$ ~ Si(O^{t}Bu)$_3$ > (c-$C_5H_9)_7Si_8O_{12}$ (SIPOSS cluster). The same order of substituent effects was obtained for $\lambda_{calc}(1a_1 \rightarrow b_2)$ calculated by DFT methods for optimized structures **2**, **4**, and **6**−**8**. Calculated natural charges for the Cp^*_2Ti moiety (equal to negative charges on OR′) increased following the order of increasing $\lambda_{calc}(1a_1 \rightarrow b_2)$, whereas the calculated delocalization energies $O(p_z) \rightarrow Ti$ displayed a reverse trend. This is in agreement with the anticipated assumption that the more polar the Ti−O bond, the weaker the covalent interaction. Calculations on compound **7** with the natural bent and collinear Ti−O−H moiety revealed that the oxygen π-donation depends only slightly on the bending angle. This was corroborated for the Ti−O−C case by analogous treatment of optimized bent and collinear Ti−O−C in **8**. The obtained order of substituent effects should be of general validity for evaluation of oxygen π-donation in titanocene Ti(IV) complexes as well as in half-sandwich titanocene complexes for catalytic application in olefin polymerization. Experiments on titanocene alkoxy-tethered compounds with a Ti−O−C angle of about 130° (Chart 1) and DFT calculations of oxygen π-donation in these compounds are under way.

Experimental Section

General Considerations. Reactions of **1** with dehydrated and degassed alcohols were carried out under vacuum on a vacuum line in sealed all-glass devices equipped with breakable seals or under an argon atmosphere. EI-MS spectra were measured on a VG-7070E mass spectrometer at 70 eV. Crystalline samples in

---

(24) (a) Besancon, J.; Top, S.; Tirouflet, J.; Dusausoy, Y.; Lecomte, C.; Protas, J. *J. Organomet. Chem.* **1977**, *127*, 153–168. (b) Köcher, S.; Walfort, B.; Rheinwald, G.; Rüffer, T.; Lang, H. *J. Organomet. Chem.* **2008**, *693*, 3213–3222. (c) Huffman, J. C.; Moloy, K. G.; Marsella, J. A.; Caulton, K. G. *J. Am. Chem. Soc.* **1980**, *102*, 3009–3014.

(25) (a) Pellny, P.-M.; Burlakov, V. V.; Baumann, W.; Spannenberg, A.; Rosenthal, U. *Z. Anorg. Allg. Chem.* **1999**, *625*, 910–918. (b) Polse, J. L.; Andersen, R. A.; Bergman, R. G. *J. Am. Chem. Soc.* **1995**, *117*, 5393–5394. (c) Bochmann, M.; Jaggar, A. J.; Wilson, L. M.; Hursthouse, M. B.; Motevalli, M. *Polyhedron* **1989**, *8*, 1838–1843.

(26) Ploom, A.; Tuulmets, A. *J. Organomet. Chem.* **2009**, *694*, 313–315.

(27) Simon, S.; Duran, M.; Dannenberg, J. J. *J. Chem. Phys.* **1996**, *105*, 11024–11031.

(28) Stroot, J.; Beckhaus, R.; Saak, W.; Haase, D.; Lützen, A. *Eur. J. Inorg. Chem.* **2002**, 1729–1737, and references therein.

(29) Varga, V.; Císařová, I.; Horáček, M.; Pinkas, J.; Kubišta, J.; Mach, K. *Collect. Czech. Chem. Commun.* **2009**, *74*, DOI: 10.1135/cccc2008212.

Chart 1

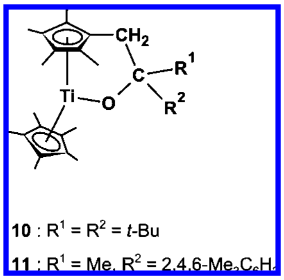

sealed capillaries were opened and inserted into the direct inlet under argon. The spectra are represented by the peaks of relative abundance higher than 7% and by important peaks of lower intensity. Crystals for EI-MS measurements and melting point determinations were placed in glass capillaries, and KBr pellets for IR spectra were pressed in a Labmaster 130 (mBraun) glovebox under purified nitrogen (concentrations of oxygen and water were lower than 2.0 ppm) and sealed with flame. IR spectra were measured in an air-protecting cuvette on a Nicolet Avatar FT IR spectrometer in the range 400−4000 cm^{-1}. X-Band EPR spectra were recorded on an ERS-220 spectrometer (Center for Production of Scientific Instruments, Academy of Sciences of GDR, Berlin, Germany) operated by a CU-3 unit (Magnettech, Berlin, Germany). *g*-Values were determined by using an Mn^{2+} standard at $g = 1.9860$ ($M_I = -1/2$ line). A STT-3 variable-temperature unit was used for measurements in the range −140 to +25 °C. UV-near IR spectra in the range 300−2000 nm were measured on a Varian Cary 17D spectrometer in all-sealed quartz cells (Hellma).

Chemicals. The solvents, hexane and toluene were dried by refluxing over LiAlH$_4$ and stored as solutions of green dimeric titanocene [(μ-η^5:η^5-C$_5$H$_4$C$_5$H$_4$)(μ-H)$_2${Ti(η^5-C$_5$H$_5$)}$_2$].[30] The single tucked-in permethyltitanocene, [Ti(III){η^5:η^1-C$_5$Me$_4$(CH$_2$)}(η^5-C$_5$Me$_5$)] (**1**), was prepared from [TiCl$_2$(η^5-C$_5$Me$_5$)$_2$] via [TiCl(η^5-C$_5$Me$_5$)$_2$], and [TiMe(η^5-C$_5$Me$_5$)$_2$] by thermolysis of the latter at 110 °C for 3 h.[19c] Commercial silanols tris(*tert*-butoxy)silanol, (Me$_3$CO)$_3$SiOH, triisopropylsilanol, (Me$_2$HC)$_3$SiOH, triphenylsilanol, (C$_6$H$_5$)$_3$SiOH, and [3,5,7,9,11,13,15-heptacyclopentylpentacyclo[9.5.1.1^{3,9}.1^{5,15}.1^{7,13}]octasiloxan-1-ol, (c-C$_5$H$_9$)$_7$Si$_7$O$_{12}$-SiOH (SIPOSS) (all Aldrich) were degassed and used as such. *tert*-Butanol (Aldrich) was dehydrated by treating with doubly tucked-in permethyltitanocene followed by vacuum distillation.[31]

Preparation of Permethytitanocene Silanolates. Compound **1** (0.50 g, 1.57 mmol) was dissolved in hexane (20 mL), and the solution mixed with a solution of the respective silanol (1.60 mmol) in hexane. The initial intense purple color of **1** turned nearly immediately to a pale pink color of the product. After stirring for 20 min the volume of the solution was reduced by vacuum distillation to make a nearly saturated solution. This was cooled to −5 or −28 °C for crystallization. The crystals were separated from the mother liquor and recrystallized from hexane. Yields were not optimized, well-defined crystals were collected for X-ray diffraction analysis, and the same material was used for EI-MS, IR, UV-near IR, and EPR characterization.

Data for **2** are as follows. Yield of green crystals was 0.55 g (72%). Mp: 180−185 °C. EI-MS (110 °C): *m/z* (relative abundance) 493 (10), 492 (17), 491 (M$^{+\bullet}$; 38), 448 ([M − Pr]$^+$; 15), 358 (18), 357 (33), 356 ([M − Cp*]$^+$; 100), 355 (15), 354 (15), 353 (14), 318 (17), 317 ([M − HOR′]$^+$; 13), 316 (11), 315 (16), 314 ([M − Cp* − C$_3$H$_6$]$^+$; 47), 272 ([M − Cp* − 2C$_3$H$_6$]$^+$; 21), 228 (11), 227 (10), 226 (10), 225 (10), 224 (13), 181 (13), 134 (10), 119 (10). IR (KBr, cm^{-1}): 2946 (s), 2908 (s), 2863 (s), 2720 (vw), 1494 (w), 1467 (m), 1450 (m), 1379 (m), 1246 (w), 1064 (vw), 1022 (w), 1011 (w), 996 (vw), 978 (vw), 897 (vs), 805 (vw), 666 (m), 633 (w), 563 (vw), 438 (m). EPR (hexane, 22 °C): $g = 1.974$, $\Delta H = 2.8$ G, a(Ti) = 8.8 G. EPR (toluene, −140 °C): $g_1 = 2.000$, $g_2 = 1.980$, $g_3 = 1.949$, $g_{av} = 1.976$. UV-near IR (hexane, nm): 505 > 650 ~ 1585. Anal. Calcd for C$_{29}$H$_{51}$OSiTi (491.68): C, 70.84; H, 10.45. Found: C, 70.80; H, 10.41.

Data for **3** are as follows. Yield of green crystals was 0.73 g (78%). Mp: 220 °C. EI-MS (200 °C): *m/z* (relative abundance) 596 (9), 595 (16), 594 (28), 593 (M$^{+\bullet}$; 46), 592 (12), 591 (10), 461 (10), 460 (24), 459 (46), 458 ([M − Cp*]$^+$; 100), 457 (26), 456 (18), 317 ([M − HOR′]$^+$; 13), 276 ([M − Cp* − SiPh$_2$]$^+$; 10), 259 ([SiPh$_3$]$^+$; 10), 258 (10), 202 (10), 201 (11), 200 (16), 199 ([M − Cp* − SiPh$_3$]$^+$; 16), 181 (11), 168 (11), 135 (26), 119 (23), 105 (17), 91 (16). IR (KBr, cm^{-1}): 3066 (w), 3047 (vw), 3009 (vw), 2995 (w), 2974 (vw), 2904 (m), 2857 (w), 2720 (vw), 1589 (vw), 1484 (w), 1451 (w), 1428 (m), 1379 (w), 1256 (vw), 1189 (vw), 1109 (s), 1030 (vw), 1002 (w), 956 (vs), 804 (vw), 744 (w), 703 (s), 514 (s), 502 (m), 420 (m). EPR (toluene, 22 °C): $g = 1.973$, $\Delta H = 2.4$ G. $a_{Ti} = 8.4$ G. EPR (toluene, −140 °C): $g_1 = 2.000$, $g_2 = 1.982$, $g_3 = 1.941$, $g_{av} = 1.974$. UV-near IR (toluene, nm): 500 > 642 ~ 1725. Anal. Calcd for C$_{38}$H$_{45}$OSiTi (593.73): C, 76.87; H, 7.64. Found: C, 76.91; H, 7.66.

Data for **4** are as follows. Yield of brownish-green crystals was 0.78 g (86%). Mp: 130 °C with decomposition. EI-MS (110 °C): *m/z* (relative abundance) 583 (17), 582 (35), 581 (M$^{+\bullet}$; 69), 580 (11), 508 ([M − OBu]$^+$; 11), 446 ([M − Cp*]$^+$; 5), 390 ([M − Cp* − C$_4$H$_8$]$^+$; 7) 389 (6), 374 ([M − OBu − C$_5$Me$_4$CH$_2$]$^+$; 10), 335 (9), 334 ([M − Cp* − 2C$_4$H$_8$]$^+$; 15), 333 (12), 319 (6), 318 (19), 317 ([M − HOR′]$^+$; 23), 280 (21), 279 (43), 278 ([M − Cp* −3C$_4$H$_8$]$^+$; 100), 277 (64), 276 (22), 262 (27), 261 (24), 260 ([M − Cp* − 3C$_4$H$_8$ − H$_2$O]$^+$; 30), 259 (19), 249 (23), 198 ([(C$_5$Me$_4$CH$_2$)TiO]$^+$; 17), 137 (33), 135 (25), 134 (20), 133 (10), 119 (20), 105 (10), 79 (24), 57 (94). IR (KBr, cm^{-1}): 2974 (s), 2927 (m), 2903 (m), 2867 (m), 2722 (vw), 1495 (vw), 1472 (w), 1444 (w), 1388 (m), 1362 (m), 1236 (m), 1215 (m), 1192 (s), 1047 (vs), 1025 (s), 964 (vs), 819 (w), 684 (m), 620 (vw), 526 (w), 495 (m), 474 (w), 438 (m), 423 (m). EPR (toluene, 22 °C): $g = 1.972$, $\Delta H = 2.6$ G, $a_{Ti} = 8.3$ G. EPR (toluene, −140 °C): $g_1 = 1.999$, $g_2 = 1.981$, $g_3 = 1.939$, $g_{av} = 1.973$. UV-near IR (hexane, nm): 318 (sh) > 374 (sh) > 497 > 665 ~ 1700. Anal. Calcd for C$_{32}$H$_{57}$O$_4$SiTi (581.76): C, 66.07; H, 9.88. Found: C, 65.98; H, 9.83.

Preparation of 5. Compound **1** (0.30 g, 0.94 mmol) was dissolved in hexane (20 mL), and the solution mixed with a solution of SIPOSS (0.86 g, 0.94 mmol) in hexane (10 mL). The initial intense purple color of **1** turned nearly immediately to a pale pink color of the product. After stirring for 30 min the volume of the reaction solution was reduced to ca. 5 mL by evaporation of hexane under vacuum, and the solution was cooled to −28 °C overnight. A pale purple crystalline solid was separated from the mother liquor and dissolved in hexane and in toluene for spectroscopic measurements. Attempts to prepare single crystals suitable for X-ray diffraction analysis failed; the crystals lost solvent of crystallization both under vacuum and in a nitrogen atmosphere.

Data for **5** are as follows. IR (KBr, cm^{-1}): 2950 (s), 2912 (w), 2866 (m), 2720 (vw), 1493 (vw), 1453 (w), 1382 (w), 1248 (w), 1117 (vs), 1038 (s), 948 (vw), 916 (w), 727 (vw), 617 (vw), 579 (vw), 509 (m), 422 (w). EPR (toluene, 22 °C): $g = 1.9714$, $\Delta H = 2.7$ G, $a_{Ti} = 8.2$ G. EPR (toluene, −140 °C): $g_1 = 2.000$, $g_2 = 1.983$, $g_3 = 1.934$, $g_{av} = 1.972$. UV-near IR (hexane, nm): 504 > 605(sh) ~ 1800.

Preparation of 6. Compound **1** (0.50 g, 1.57 mmol) was dissolved in hexane (20 mL), and *t*-BuOH (0.2 mL, 2.10 mmol) was added. The initial intense purple color of **1** became immediately less intense. The reaction solution was evaporated under vacuum to remove hexane with excess *t*-BuOH, and a purple residue was

---

[30] Antropiusová, H.; Dosedlová, A.; Hanuš, V.; Mach, K. *Transition Met. Chem. (London)* **1981**, *6*, 90–93.

[31] Pinkas, J.; Gyepes, R.; Císařová, I.; Horáček, M.; Štěpnička, P.; Kubišta, J.; Varga, V.; Mach, K. *Collect. Czech. Chem. Commun.* **2008**, *73*, 967–982.

Table 3. Crystallographic Data and Data Collection and Structure Refinement Details for 2−4 and 6

	4	**3**	**2**	**6**
formula	$C_{32}H_{57}O_4SiTi$	$C_{38}H_{45}OSiTi$	$C_{29}H_{51}OSiTi$	$C_{24}H_{39}OTi$
mol wt	581.77	593.73	491.69	391.45
cryst syst	triclinic	orthorhombic	triclinic	monoclinic
space group	$P\bar{1}$ (No. 2)	$Pbca$ (No. 61)	$P\bar{1}$ (No. 2)	$P2_1/c$ (No. 14)
a (Å)	10.5233(2)	20.6532(2)	11.8550(3)	14.89220(10)
b (Å)	11.1081(2)	14.3925(2)	14.9147(4)	10.8752(2)
c (Å)	15.3903(3)	22.6067(3)	16.2430(4)	14.7644(2)
α (deg)	83.5103(11)	90	92.0898(13)	90
β (deg)	87.7159(11)	90	90.2051(16)	109.4532(9)
γ (deg)	69.6085(10)	90	94.6256(16)	90
V (Å^3)	1675.49(5)	6719.87(14)	2860.67(13)	2254.67(5)
Z	2	8	4	4
D_{calcd} (g cm^{-3})	1.153	1.174	1.142	1.153
μ (mm^{-1})	0.323	0.318	0.359	0.389
color	brown-green	green	green	purple
cryst size (mm^3)	0.5 × 0.4 × 0.3	0.5 × 0.4 × 0.2	0.5 × 0.25 × 0.16	0.5 × 0.4 × 0.36
T (K)	150(2)	150(2)	150(2)	150(2)
θ_{min}; θ_{max} (deg)	1.33; 27.57	1.95; 27.48	1.82; 25.10	2.93; 27.51
range of h	−13/13	−26/26	−14/14	−19/19
range of k	−14/14	−18/18	−17/17	−14/14
range of l	−19/19	−29/29	−0/19	−19/19
no. of rflns collected	36 181	84 166	40 988	49 598
no. of unique reflns	7713	7704	10 062	5179
F(000)	634	2536	1076	852
no. of params refined	362	380	611	248
$R(F)$; $wR(F^2)$ all data (%)	4.07; 9.01	6.59; 11.68	7.84; 16.84	3.58; 9.02
GooF (F^2), all data	1.026	1.035	1.121	1.040
$R(F)$; $wR(F^2)$ ($I > 2\sigma(I)$) (%)	3.37; 8.52	4.22; 10.26	6.54; 16.00	3.20; 8.73
$\Delta\rho$ (e Å^{-3})	0.291; −0.473	0.367; −0.321	0.867; −0.451	0.311; −0.258

dissolved in 5 mL of hexane. The solution was cooled to −28 °C for 2 days, and a mass of purple crystals was separated from the mother liquor. The crystals were recrystallized from a minimum of hexane to give small needle crystals for X-ray diffraction analysis and spectroscopic characterization. The mother liquor after a partial evaporation of hexane afforded another crop of purple crystals that gave the same spectral data as the recrystallized ones. Total yield: 0.50 g (82%).

Data for **6** are as follows. Mp: 122 °C. EI-MS (80 °C): *m/z* (relative abundance) 393 (16), 392 (41), 391 ($M^{+\bullet}$; 95), 390 (17), 389 (15), 336 (23), 335 ($[M - C_4H_8]^+$; 84), 334 (20), 319 (26), 318 (75), 317 ($[M - HOR']^+$; 100), 316 (30), 315 (26), 257 (16), 256 ($[M - Cp^*]^+$; 64), 255 (31), 241 (21), 240 ($[M - Cp^* - CH_4]^+$; 90), 239 (28), 201 (20), 200 (89), 199 (45), 198 (33), 196 (13), 195 (30), 183 (23), 182 (90), 181 (48), 180 (54), 179 (19), 178 (34), 177 (17), 119 (13). IR (KBr, cm^{-1}): 3002 (m,sh), 2964 (s), 2906 (vs), 2862 (m), 2720 (vw), 1499 (w), 1439 (m,b), 1378 (s), 1351 (m), 1208 (m), 1182 (vs), 1062 (vw), 1022 (m), 985 (vs), 803 (vw), 775 (m), 528 (m), 482 (vw), 462 (w). EPR (hexane, 22 °C): $g = 1.978$, $\Delta H = 2.7$ G, $a_{Ti} = 8.5$ G. EPR (toluene, −140 °C): $g_1 = 2.000$, $g_2 = 1.980$, $g_3 = 1.957$, $g_{av} = 1.979$. UV-near IR (hexane, nm): 525 > ~650 (sh) > ~1300. Anal. Calcd for $C_{24}H_{39}OTi$ (391.44): C, 73.64; H, 10.04. Found: C, 73.56; H, 10.00. The IR and EPR data agree with those reported.[32]

Computational Details. DFT studies have been carried out at the Fermi cluster at the J. Heyrovský Institute of Physical Chemistry, Academy of Sciences of Czech Republic, v.v.i., using Gaussian 03, revision E.01.[33] All calculations used the Becke exchange[34] and the Perdew/Wang 91 correlational functionals.[35] The geometries of **2**, **4**, and **6** were optimized using the 6-311G(3d,p) basis set and those of **7** and **8** using the 6-311G(d,p) basis set employed for all atoms and an analytical Hessian computed before the first step of the optimization procedure. Numerical integration was done on a pruned grid having 99 radial shells each of 590 angular points. Natural bonding analysis[36] was carried out by the NBO 3.1 program integrated in Gaussian.[37] Mayer bond order[38] determination and natural bonding analysis were carried out employing only the 6-31+G(d,p) basis set on the optimized geometries of **2**, **4**, and **6**−**8**. The electronic transitions were computed by time-dependent DFT[39] using the relativistic effective potential of Hurley et al.[40] for Ti, the potential of Pacios and Christiansen[41] for Si (if applicable), and the 6-31++G(d,p) basis set for all other atoms against the same geometries as the bond order analyses. Visualization and examination of molecular orbitals was accomplished by Molden.[42]

X-ray Crystallography. Single crystals or crystal fragments of **2**−**5** were mounted on Lindemann glass capillaries in a Labmaster 130 glovebox (mBraun) under purified nitrogen. Diffraction data for all complexes were collected on a Nonius KappaCCD diffractometer (Mo Kα radiation, $\lambda = 0.71073$ Å) and processed by the HKL program package.[43] The phase problem was solved by direct methods (SIR97),[44] followed by consecutive Fourier syntheses, and refined by full-matrix least-squares on F^2 (SHELXL-97).[45] Relevant

---

(32) Pattiasina, J. W.; Heeres, H. J.; van Bolhuis, F.; Meetsma, A.; Teuben, J. H.; Spek, A. L. *Organometallics* **1987**, *6*, 1004–1010.

(33) Frisch, M. J.; et al. *Gaussian 03, Revision E.01*; Gaussian, Inc.: Wallingford, CT, 2004.

(34) Becke, A. D. *Phys. Rev. A* **1988**, *38*, 3098–3100.

(35) Perdew, J. P.; Burke, K.; Wang, Y. *Phys. Rev.* **1996**, *B54*, 16533–16539.

(36) Carpenter, J. E.; Weinhold, F. *J. Mol. Struct. (THEOCHEM)* **1988**, *169*, 41–62.

(37) Glendening, E. D.; Badenhoop, J. K.; Reed, A. E.; Carpenter, J. E.; Weinhold, F. *NBO Version 3.1*; Theoretical Chemistry Institute, University of Wisconsin: Madison, WI.

(38) Bridgemann, A. J.; Cavigliasso, G.; Ireland, L. R.; Rothery, J. *J. Chem. Soc., Dalton Trans.* **2001**, 2095–2108.

(39) Stratmann, R. E.; Scuseria, G. E.; Frisch, M. J. *J. Chem. Phys.* **1998**, *109*, 8218–8224.

(40) Hurley, M. M.; Pacios, L. F.; Christiansen, P. A.; Ross, R. B.; Ermler, W. C. *J. Chem. Phys.* **1986**, *84*, 6840–6853.

(41) Pacios, L. F.; Christiansen, P. A. *J. Chem. Phys.* **1985**, *82*, 2664–2671.

(42) Schaftenaar, G.; Noordik, J. H. Molden: a pre- and post-processing program for molecular and electronic structures. *J. Comput.-Aided Mol. Des.* **2000**, *14*, 123–134.

(43) Otwinowski, Z.; Minor, W. HKL Denzo and Scalepack program package by Nonius. *Methods Enzymol.* **1997**, *276*, 307–326.

(44) Altomare, A.; Burla, M. C.; Camalli, M.; Cascarano, G.; Giacovazzo, C.; Guagliardi, A.; Polidori, G. *J. Appl. Crystallogr.* **1994**, *27*, 435–436.

crystallographic data are given in Table 3. All non-hydrogen atoms were refined anisotropically. Hydrogen atoms were included in idealized positions and refined isotropically using the riding model. Molecular graphics was carried out with the PLATON program.[46]

Acknowledgment. This research was supported by the Academy of Sciences of the Czech Republic (Grant No. KAN100400701) and the Ministry of Education, Youth and Sports (Project No. LC06070), I.C. and R.G. are grateful to MSM0021620857.

Supporting Information Available: CIF file for structures **2**, **3**, **4**, and **6**. UV-near IR spectra of **2**−**6**, supporting information and PLATON drawing at 30% probability for structures **2**, **3**, **4**, and **6**, correlation diagram for bent **7**, α orbital energies for **7**, molecular orbitals from correlation diagram, and the full ref 33. This material is available free of charge via the Internet at http://pubs.acs.org.

OM801209F

---

(45) Sheldrick, G. M. *SHELXL97, Program for Crystal Structure Refinement from Diffraction Data*; University of Göttingen: Göttingen, 1997.

(46) Spek, A. L. *PLATON, A Multipurpose Crystallographic Tool*; Utrecht University: Utrecht, The Netherlands, 2007.